Disulfide bond formation through Cys186 facilitates functionally relevant dimerization of trimeric hyaluronan-binding protein 1 (HABP1)/p32/gC1qR

Babal Kant Jha[1], Dinakar M. Salunke[2] and Kasturi Datta[1]

[1]*Biochemistry Laboratory, School of Environmental Sciences, Jawaharlal Nehru University, New Delhi, India;*
[2]*Structural Biology Unit, National Institute of Immunology, Aruna Asaf Ali Marg, New Delhi, India*

Hyaluronan-binding protein 1 (HABP1), a ubiquitous multifunctional protein, interacts with hyaluronan, globular head of complement component 1q (gC1q), and clustered mannose and has been shown to be involved in cell signalling. *In vitro,* this recombinant protein isolated from human fibroblast exists in different oligomeric forms, as is evident from the results of various independent techniques in near-physiological conditions. As shown by size-exclusion chromatography under various conditions and glutaraldehyde cross-linking, HABP1 exists as a noncovalently associated trimer in equilibrium with a small fraction of a covalently linked dimer of trimers, i.e. a hexamer. The formation of a covalently-linked hexamer of HABP1 through Cys186 as a dimer of trimers is achieved by thiol group oxidation, which can be blocked by modification of Cys186. The gradual structural transition caused by cysteine-mediated disulfide linkage is evident as the fluorescence intensity increases with increasing Hg^{2+} concentration until all the HABP1 trimer is converted into hexamer. In order to understand the functional implication of these transitions, we examined the affinity of the hexamer for different ligands. The hexamer shows enhanced affinity for hyaluronan, gC1q, and mannosylated BSA compared with the trimeric form. Our data, analyzed with reference to the HABP1/p32 crystal structure, suggest that the oligomerization state and the compactness of its structure are factors that regulate its function.

Keywords: clustered mannose; hyaluronan; hyaluronan-binding protein 1 (HABP1); oligomerization; p32.

Hyaluronan-binding protein 1 (HABP1), a 68-kDa protein, was originally purified as a novel receptor of hyaluronan, an important component of the extracellular matrix [1]. Subsequently, we characterized the protein and confirmed its localization on the cell surface [2] and its role in cell adhesion and tumour invasion [3], sperm maturation, and motility [4,5]. The role of this protein in hyaluronan-mediated cellular signalling is well documented, as hyaluronan binding to lymphocyte and hyaluronan-mediated lymphocyte aggregation were inhibited by pretreatment of the cells with antibodies to HABP1 [6]. This is further strengthened by the observation of enhanced phosphorylation of HABP1 and increased formation of inositol trisphosphate and phospholipase C-γ in hyaluronan-supplemented cells, which have been shown to be inhibited by pretreatment with antibodies to HABP1 [7]. As a continuation of this study, the cDNA encoding HABP from human skin fibroblast has been cloned and sequenced [8]. The presence of the hyaluronan-binding motif was confirmed and the overexpressed protein subsequently shown to bind hyaluronan. The gene encoding this protein has been assigned to human chromosome 17p12-p13 and has been named HABP1 [9]. A computer search of the sequence encoding HABP1 revealed identity with p32, a protein copurified with splicing factor SF2 [10], and with the receptor for globular head of complement subcomponent C1q (gC1qR) [11], and substantial homology (92%) with YL-2, the HIV-rev binding murine homologue [12,13].

Recent studies on p32/HABP1 show its localization in various cellular compartments including mitochondria, nucleus, cytosol and the cell surface in different cell types [14,15]. In addition, interaction of p32/HABP1 with a number of proteins, including hepatitis C virus core protein, which inhibits T-lymphocyte proliferation [16], *Staphylococcus aureus* protein A [17], *Listeria monocytogenes* protein In1B [18], high-molecular-mass kininogen [19], clustered mannose [20] and lamin B receptor [21] give new dimensions to the actual functional role of p32/HABP1. The crystal structure of p32/HABP1 shows a solvent-exposed hyaluronan-binding motif in its trimeric assembly [22]. Interaction of this protein with many different ligands suggests the existence of different molecular forms. In addition to a tightly coupled receptor–ligand interaction, its biological specificity and function are regulated by intricate mechanisms involving conformational transitions in several proteins [23]. However, the structural flexibility of HABP1 in solution has not been addressed adequately. In this study, we have examined the structural transitions of HABP1 and the effects of these on affinity for different ligands.

MATERIALS AND METHODS

Materials

EAH–Sepharose 4B, Superose 6 columns, Sephadex G-25 and molecular mass markers were obtained from Pharmacia Biotech Inc. (Uppsala, Sweden). The Protoblot Western-blot system was purchased from Promega Corp. (Madison, WI, USA). ImmunoPure Biotin-LC-Hydrazide was purchased from Pierce (Rockford, IL, USA). Complement component 1q (C1q) and the other chemicals were obtained from Sigma Chemicals Co. (St Louis, MO, USA).

Purification of HABP1 and preparation of its polyclonal antibodies

HABP1 was purified to homogeneity using ion-exchange chromatography on a Mono Q HR $10/10^{TM}$ column (Pharmacia), interfaced with a Pharmacia $FPLC^{TM}$ system using a linear gradient of 0–1 M NaCl in 20 mM Hepes, pH 7.5, containing 1 mM EDTA, 1 mM EGTA, 5% glycerol and 0.2% 2-mercaptoethanol, followed by hyaluronan–Sepharose affinity column chromatography as reported previously [8] and size-exclusion chromatography in 10 mM phosphate-buffered saline containing 150 mM NaCl. Antibodies to purified HABP1 were raised in a New Zealand White rabbit [8].

Electrophoresis and immunodetection

Gradient or linear polyacrylamide slab gel electrophoresis was carried out by the procedure of Laemmli [24]. HABP1 that had undergone different treatments was also subjected to either 9% nondenaturing PAGE or pore-limiting gel electrophoresis on polyacrylamide gel of gradient 7–24% as described previously, with the modification of 0.005% SDS in Tris/glycine running buffer, pH 8.3 [25,26]. Separated proteins were transferred to nitrocellulose membrane by applying current at $0.8 \ mA \cdot cm^{-2} \cdot h^{-1}$ in a semidry transfer unit (Pharmacia); they were immunodetected using rabbit anti-HABP1 IgG (1 : 1000 dilution) visualized by the nitro blue tetrazolium (NBT)/5-bromo-4-chloro-3-indolyl phosphate (BCIP) detection system using alkaline phosphatase conjugated goat anti-(rabbit IgG) Ig as secondary antibody (1 : 7500 dilution).

Gel-permeation chromatography of HABP1

Gel-permeation chromatography was carried out on a Pharmacia Superose 6^{TM} analytical column (1 × 30 cm) interfaced with an $FPLC^{TM}$ system at a flow rate of $0.3 \ mL \cdot min^{-1}$. The buffer was 10 mM phosphate, pH 7.2, with or without 0.1% (v/v) 2-mercaptoethanol and/or 0.1% (w/v) sodium lauryl sulfate, keeping the ionic concentration constant at 150 mM NaCl. The standard molecular mass markers of known molecular mass and Stokes radius, alcohol dehydrogenase (150 kDa, 46 Å); BSA (67 kDa, 35.5 Å); ovalbumin (43 kDa, 30.5 Å) chymotrypsinogen (25 kDa, 20.9 Å) and ribonuclease A (13.7 kDa, 16.4 Å) were independently run in each case.

Chemical modification of HABP1

Chemical modification of the cysteine residue was carried out as reported previously [27]. In brief, HABP1 $(1 \ mg \cdot mL^{-1})$ was treated with iodoacetamide and iodoacetic acid (1 : 3 molar ratio) in 50 mM Tris/HCl, pH 8.5, containing 1 mM EDTA, 1 mM EGTA, 10 mM dithiothreitol and 8 M urea at room temperature for 30 min. This reaction mixture was passed through a Sephadex G-25 column, and the protein fractions were pooled and concentrated for use as cysteine-modified HABP1.

Covalent cross-linking of HABP1 subunits

To HABP1 (0.2 μM) in 10 mM phosphate buffer, pH 7.2, containing 150 mM NaCl, an aliquot of 25% (mass/volume) glutaraldehyde was added to a final concentration of 1%. This sample was incubated at 25 °C for 5 min; the cross-linking reaction was then quenched by adding 30 mM 1-mercaptoethanol [28]. After 20 min of incubation, 10% (w/v) aqueous sodium deoxycholate stock was added to the reaction mixture to a final concentration of 0.3%. The pH of the reaction mixture (in 10 mM phosphate, 150 mM NaCl, pH 7.2) was lowered to 2.0–2.5 by the addition of concentrated orthophosphoric acid, which resulted in coprecipitation of cross-linked HABP1 with sodium deoxycholate. After centrifugation (13 327 *g*, 4 °C), the precipitate was redissolved in 0.1 M Tris/HCl, pH 8.0, containing 1% SDS and 0.1% 2-mercaptoethanol and heated at 90–100 °C for 3 min. This sample was separated by SDS/PAGE (12.5% gel), transferred to nitrocellulose membrane, immunodetected using rabbit anti-HABP1 IgG, and visualized by the NBT/BCIP detection system.

Copper–phenanthroline-induced disulfide linkage of HABP1

Catalytic oxidation of the thiol group of HABP1 was achieved with a copper–phenanthroline complex [29]. Purified HABP1 $(1 \ mg \cdot mL^{-1})$ in $NaCl/P_i$ was incubated with one-tenth reaction volume of 2.5 mM $CuSO_4 \cdot 5H_2O$ and 5 mM 1,10-phenanthroline. The mixture was gently vortex-mixed under aerobic conditions, incubated for 10 min at room temperature, and passed through a Sephadex G-25 column; protein-containing fractions were pooled and concentrated using a $Centricon^{TM}$ membrane (10-kDa cut-off). The concentrated protein was mixed with native-PAGE sample buffer and analyzed on a native 9% polyacrylamide gel. The same sample was analyzed for copper on a PU2000X Philips atomic absorption spectrometer with a sensitivity of ≈ 0.3 μM using copper nitrate as standard solution.

$HgCl_2$-induced disulfide linkage of HABP1

$HgCl_2$-induced disulfide linkage of two cysteine residues was achieved by a previously described procedure [30]. Purified HABP1 $(1 \ mg \cdot mL^{-1})$ in $NaCl/P_i$ was incubated with $HgCl_2$ at a concentration of 50 μM at 30 °C for 10 min. Aliquots were mixed with native-PAGE sample buffer and analyzed by native PAGE (9% gel) or pore-limiting PAGE.

Estimation of thiol group

The Ellman assay was performed to determine the free thiol group in HABP1, cysteine-modified and copper–phenanthroline-oxidized HABP1 as previously described [27]. In brief, 800 μL protein solution (10 μM) in 10 mM phosphate buffer containing 150 mM NaCl, 1 mM EDTA and 6 M guanidinium hydrochloride (pH 7.2) was placed in the sample compartment of a spectrophotometer (Cary100; Varian Inc.) interfaced with a Peltier temperature controller; the reference compartment contained buffer only. The absorbance difference at 412 nm was set to zero at 25 °C. Then, 40 μL 5,5′-dithionitrobenzoic acid was added to the sample and reference compartments of each cuvette, and the contents thoroughly mixed. The absorbance difference at 412 nm was immediately monitored, and the value recorded when there was no further increase. The thiol molar concentration was calculated from the increased absorbance caused by 5,5′-dithionitrobenzoic acid taking the molar absorbance of the thionitrobenzoate anion to be $\varepsilon_{412} = 13\ 700$ in 6 M guanidinium hydrochloride.

Fluorescence measurement

HgCl$_2$-treated HABP1 was passed through a Sephadex G-25 column to remove free Hg^{2+} ion and concentrated using a Centricon^{TM} membrane (10-kDa cut-off) in 20 mM Tris/HCl, pH 7.5, buffer to 0.2 mg·mL^{-1} so that $A_{282} \leq 0.1$ to avoid any inner-filter effect. the sample was excited at 282 nm; the excitation maxima of HABP1 and emission were collected at 347 nm on a PerkinElmer LS50B fluorimeter. The background emission intensity was subtracted using the buffer alone.

Biotinylation of hyaluronan, D-mannosylated BSA and HABP1, and their use in binding assays

Hyaluronan was biotinylated by the procedure of Yang *et al.* [31]. HABP1 and the polypeptide backbone of mannosylated BSA were biotinylated according to the instructions given for protein biotinylation in the manufacturer's (Pierce) guide, and used for the ligand-binding assay. The bound biotinylated hyaluronan, mannosylated BSA or HABP1 were probed with horseradish peroxidase-conjugated streptavidin (1 : 7500) and visualized with 2,2′-azino-bis(3-ethylbenzthiazoline-6-sulfonic acid). Alternatively, for C1q binding, it was coated on a microtitre plate and incubated with different oligomeric forms of HABP1 for 1 h at room temperature and probed with anti-HABP1 IgG; it was detected with horseradish peroxidase-conjugated goat anti-(rabbit IgG) Ig and visualized with 2,2′-azino-bis (3-ethylbenzthiazoline-6-sulfonic acid).

## RESULTS

Existence of two oligomeric forms of HABP1

The oligomeric states of HABP1 were investigated under native conditions by immunoblot analysis using antibody raised against purified rabbit HABP1. As shown in Fig. 1, different amounts of purified HABP1 in the absence of any reducing agent were subjected to native PAGE (9% gel), transferred to a nitrocellulose membrane, and immuno-
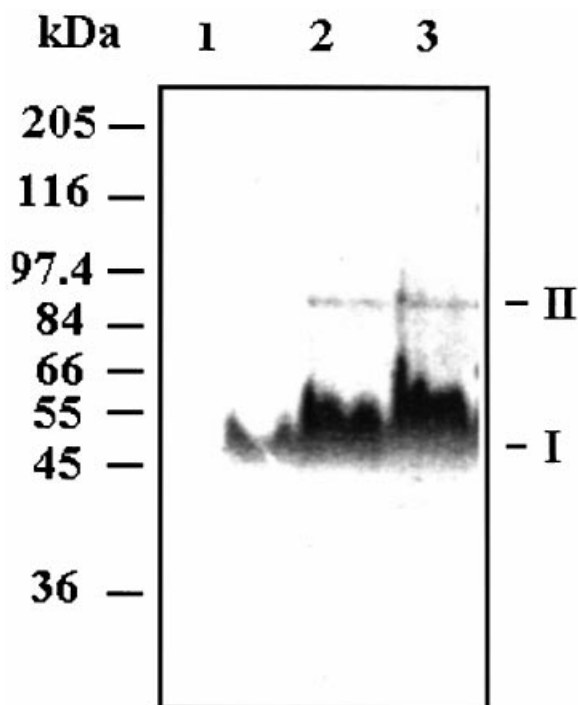
Fig. 1. HABP1 exists in two different oligomeric forms in solution. HABP1 (2 μg, lane 1; 5 μg, lane 2; 10 μg, lane 3) was electrophoresed on 9% native polyacrylamide gel in the absence of reducing agents using a discontinuous buffer system, and transferred to nitrocellulose membrane, probed with anti-HABP1 IgG, and detected using alkaline phosphatase conjugate of goat anti-rabbit IgG and an NBT/BCIP detection system. The two oligomeric forms of HABP1 are marked I and II. Molecular mass standards are shown on the left.

detected with anti-HABP1 IgG. It showed two bands, a broad and relatively prominent lower band (I) and a fairly sharp minor higher band (II). The emergence of the higher band seems to be concentration dependent *in vitro*, as it appears only in lanes 2 and 3 (Fig. 1), in which the amount of protein loaded was 5 and 10 μg, respectively. The electrophoretic mobility of band II seems to be slightly less than double that of band I. This is because HABP1 has a larger than average number of polar amino-acid residues and therefore it shows anomalous migration on PAGE. Dimerization of trimers may also change the size and conformation of the molecule, and this may be one reason why a dimer of trimers does not seem to migrate at twice the molecular mass of trimeric HABP1. The concentrations of the two oligomeric populations, estimated by densitometric comparison of the intensities of the two bands, were observed to be in the ratio of $\approx 12 : 1$.

Studies on the oligomeric transitions of HABP1 under native, reducing, and denaturing conditions were carried out by analysing their relative molecular masses using gel-permeation chromatography. Under native conditions (Fig. 2A, dotted line), HABP1 showed a major peak corresponding to a protein of apparent molecular mass 68 kDa (marked III, Fig. 2A) and a minor peak of protein corresponding to an apparent molecular mass of 136 kDa (marked IV, Fig. 2A). Thus, HABP1 exists in solution predominantly as a trimeric (68 kDa) molecule with a minor hexameric (136 kDa) form, assuming a cDNA-derived
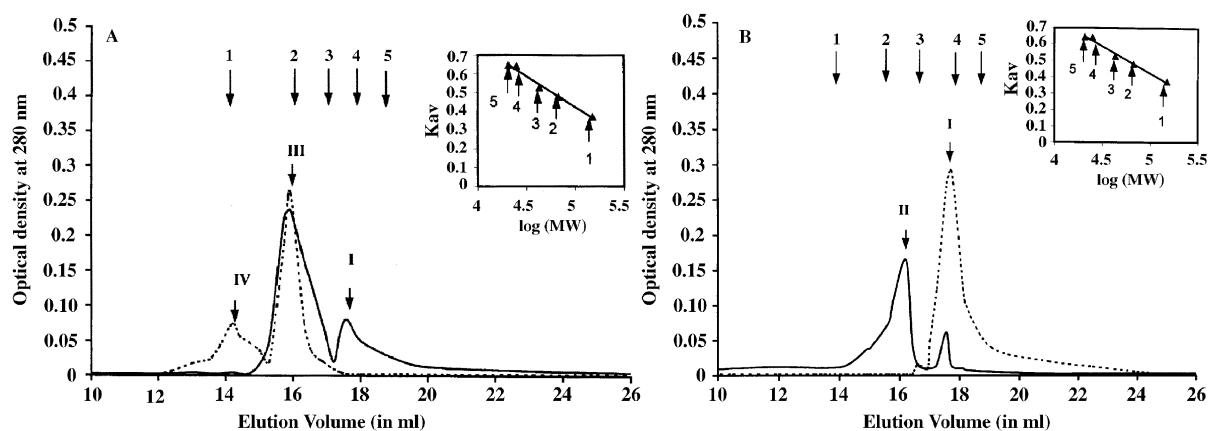
Fig. 2. Oligomeric states of HABP1 in solution. (A) Gel-permeation chromatography of HABP1 (1.2 mg·mL^{-1}) on a Superose 6 column (1 × 30 cm) in NaCl/P$_i$/0.15 M NaCl, pH 7.2 (broken line) and NaCl/P$_i$/0.15 M NaCl, pH 7.2, containing 0.1% 2-mercaptoethanol (solid line) at a flow rate of 0.3 mL·min^{-1}. The column was calibrated using molecular mass standards run under similar conditions: 1, alcohol dehydrogenase; 2, BSA; 3, ovalbumin; 4, chymotrypsinogen; 5, ribonuclease A. The estimation of the molecular mass (M_r) of the oligomer, indicated by arrows, is shown in the inset. (B) Gel-permeation chromatography of HABP1 (1.2 mg·mL^{-1}) on a Superose 6 column (1 × 30 cm) in NaCl/P$_i$/0.15 M NaCl, pH 7.2, containing 0.1% SDS (solid line) and 0.1% SDS and 0.1% 2-mercaptoethanol (broken line). The column was calibrated using the same molecular mass standards under the above conditions. The molecular mass (M_r) of standards indicated by arrows is shown in the inset and numbered 1, 2, 3, 4 and 5, respectively. The peaks marked I, II, III and IV represent monomer, dimer, trimer and hexamer, respectively.

molecular mass of 23801.1 Da for the monomer. HABP1 exists in different oligomeric forms under reducing conditions compared with native conditions. As shown in Fig. 2A (solid line), the protein in the presence of 0.1% 2-mercaptoethanol exhibited a different elution profile, although it showed two peaks, one minor (marked I, Fig. 2A) and the other major (marked III, Fig. 2A). The protein corresponding to the major peak in this case has a molecular mass of 68 kDa, and the protein of the minor peak has a molecular mass of 25 kDa, corresponding to the monomeric size of HABP1. Gel-permeation experiments carried out in the presence of 0.1% SDS and 0.1% 2-mercaptoethanol (dotted line, Fig. 2B) showed a single molecular form corresponding to a molecular mass of 25 kDa (marked I) on the basis of protein standards run under identical conditions. This clearly implies that the protein remains in the monomeric form under reducing and denaturing conditions. However, in the absence of 2-mercaptoethanol, the 25-kDa protein becomes very small and a new form corresponding to 46 kDa (marked II, Fig. 2B) appears, suggesting that, under nonreducing denaturing conditions, the protein predominantly exists in the dimeric form. On the Superose 6 column, the major peak (marked III) was eluted with a K_{av} of 0.499, which is equivalent to a Stokes radius of 36.2 Å, and the minor peak (marked IV) was eluted with a K_{av} of 0.412, which is equivalent to a Stokes radius of 46.0 Å.

To stabilize the potential oligomeric states of HABP1, the covalent cross-linker, glutaraldehyde, was incubated with HABP1 as described in Materials and methods and analysed under reducing conditions by SDS/PAGE; this was followed by transfer to a nitrocellulose membrane and immunodetection using anti-HABP1 IgG (Fig. 3A). It shows conversion of most of the monomeric band at 34 kDa to a higher species with a relative molecular mass of nearly 70 kDa. However, a smear at ≈ 20–25 kDa was consistently observed, which represents uncross-linked HABP1 monomer corresponding to the sequence-derived

molecular mass that may arise from modified electrophoretic mobility as a result of neutralization of positive charges of the lysine side chain by glutaraldehyde.

Oligomeric transitions

As is evident from the cDNA sequence, each protomer has only one cysteine (Cys186) in the polypeptide chain of HABP1 [8]. Therefore, the trimer has three free cysteine residues, which can form disulfide bonds by association with a set of three cysteine residues from another trimer leading to formation of a hexamer. However, it is also possible that, under air oxidation, the cross-linking of these cysteine residues may lead to the formation of a small proportion of hexamer. To investigate this, HABP1 was incubated with the thiol-group-oxidizing agent, Cu^{2+}−1,10-phenanthroline. There was a 100% shift of band I to band II (Fig. 3B, lane 1).

To confirm that the trimer–hexamer transition does indeed occur through disulfide linkage of cysteine residues, experiments were carried out with cysteine-modified HABP1. Gel-permeation chromatography of cysteine-modified HABP1 (Fig. 4A) shows a single peak corresponding to 68 kDa. The effect of Cu^{2+} and Hg^{2+} ions on cysteine-modified HABP1 was examined by pore-limiting PAGE to examine the role of the metal ion, if any, in disulfide bond formation. Native, cysteine-modified and HgCl$_2$-treated HABP1 were separated, transferred to nitrocellulose membrane, and probed with anti-HABP1 IgG. The data indicate dimerization of trimers, which is inhibited by cysteine modification (Fig. 4B, lane 4). To examine the molecular transition of HABP1 by HgCl$_2$, native HABP1 was treated with increasing concentrations of Hg^{2+} and subsequently desalted on a Sephadex G-25 column before monitoring of their intrinsic fluorescence. The gradual increase in fluorescence intensity with increasing Hg^{2+} concentration until all the trimeric HABP1 was presumably converted into hexameric species indicates a
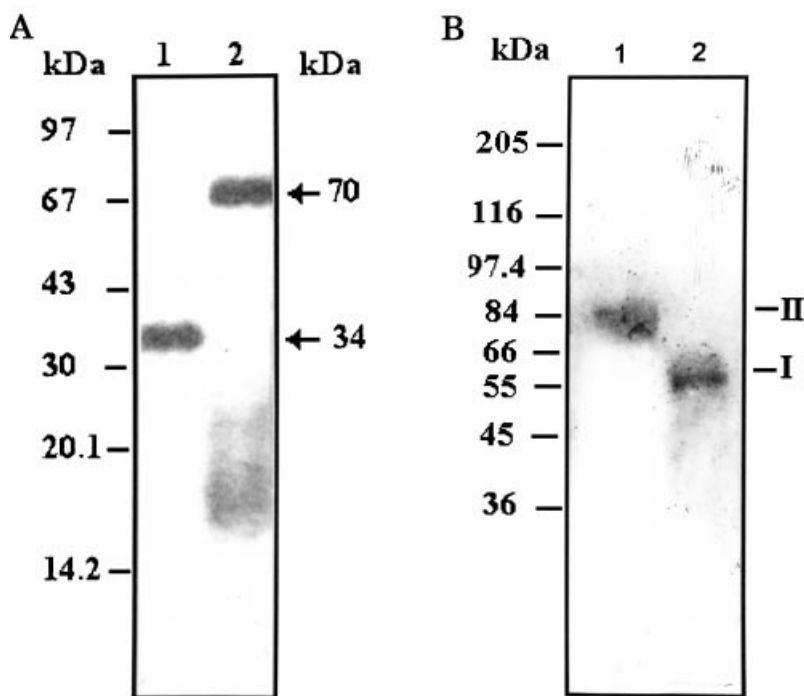
Fig. 3. Evidence for oligomeric structural transition of HABP1. (A) HABP1 was incubated with glutaraldehyde, as described in Materials and methods. The cross-linked samples were analyzed by SDS/PAGE (12.5% gel). The electrophoresed gel was transferred to nitrocellulose membrane, probed with anti-HABP1 IgG, and detected using alkaline phosphatase conjugate of goat anti-rabbit IgG and an NBT/BCIP detection system Lane 1, untreated HABP1; lane 2, treated with glutaraldehyde. The molecular mass standards are shown on the left. (B) HABP1 was incubated with $CuSO_4$ and 1,10-phenanthroline (1 : 2 molar ratio) for disulfide linkage following the earlier procedure. HABP1 alone (lane 2), and in the presence of the copper–phenanthroline complex (lane 1) were analyzed on a 9% nondenaturing gel. The gel was transblotted on a nitrocellulose membrane and probed with anti-HABP1 IgG. Molecular mass markers are shown on the left.

change in the microenvironment around tryptophan as a result of trimer dimerization (Fig. 4C).

Attempts to generate the dimer of trimers using cysteine-modified HABP1 and copper–phenanthroline as oxidant also failed; however, the unmodified form was observed to dimerize after treatment with 50 μM copper–phenanthroline (data not shown). To examine the role of metal ions in trimer dimerization, we measured the amount of copper bound to the dimer of trimers, if any, using atomic absorption spectroscopy. A protein concentration of 50 μM was used for detection of the metal ion. The data show that the copper content of this preparation is less than 15 : 1 (protein to metal ion molar ratio) keeping the detection limit of the instrument in the mind. The presence of any copper below this level is insignificant as far as trimer dimerization is concerned. Thus, the role of cysteine in trimer dimerization seems to be unambiguous.

To further establish the role of the cysteine residue in the generation of dimers of trimers, the free thiols were determined in HABP1, copper–phenanthroline-induced dimer of trimers, and cysteine-modified HABP1. No free thiol groups were available in copper–phenanthroline-induced dimer of trimers and cysteine-modified HABP1, but one free thiol group per HABP1 monomer was detected in reduced unmodified HABP1.

Oligomeric transitions and ligand affinity

The affinity of the trimeric and hexameric forms of HABP1 for its various ligands, e.g. hyaluronan, D-mannosylated BSA and gC1q, was analyzed by ELISA. $HgCl_2$ and copper–phenanthroline treatment of HABP1 resulted in trimer to hexamer conversion, which could be blocked by cysteine modification. These oligomeric forms of HABP1 were separated using size-exclusion chromatography and quantitatively analyzed for binding to biotinylated hyaluronan, biotinylated D-mannosylated BSA, and gC1q. The hexamer generated by thiol-group oxidation of native HABP1 had greater affinity for its ligand than native and cysteine-modified HABP1 or native HABP1 (Fig 5A,B,C). However, the cysteine-modified HABP1, which cannot be converted into hexamer by thiol-group oxidation, showed similar affinity for its ligands to the unmodified protein. The trimeric form of HABP1 had less affinity than the hexamer. The differential binding of trimer and hexamer was more pronounced in the case of hyaluronan than gC1q or mannosylated BSA. Therefore, the dissociation constant for the hyaluronan–HABP1 interaction was calculated by Scatchard plot analysis from the data in Fig. 5A, taking the average molecular mass of hyaluronan to be 10 MDa (Fig. 5D). The apparent dissociation constant of the hexamer was found to be 0.05×10^{-9} compared with 0.1×10^{-9} for the trimer.

DISCUSSION

In this study, we demonstrate the presence of different oligomeric forms of HABP1: monomer, noncovalently linked trimer, and cysteine-linked dimer of trimers. Interestingly, all these species of HABP1 have different affinities for hyaluronan, suggesting a possible role for different oligomeric states of HABP1 in hyaluronan signalling. The major peak on gel-filtration chromatography corresponds to the trimer of HABP1, with an estimated molecular mass of 68 kDa. This is also identical with the gel-filtration-derived molecular mass of HABP1 purified from tissue [3]. A small proportion of the protein exists in the hexameric state in solution through Cys186-linked disulfide bonds. However, the crystal structure of HABP1 in the presence of 600 mM NaCl under reducing conditions suggested that HABP1 is a trimeric protein [22]. This is in agreement with our data in solution under
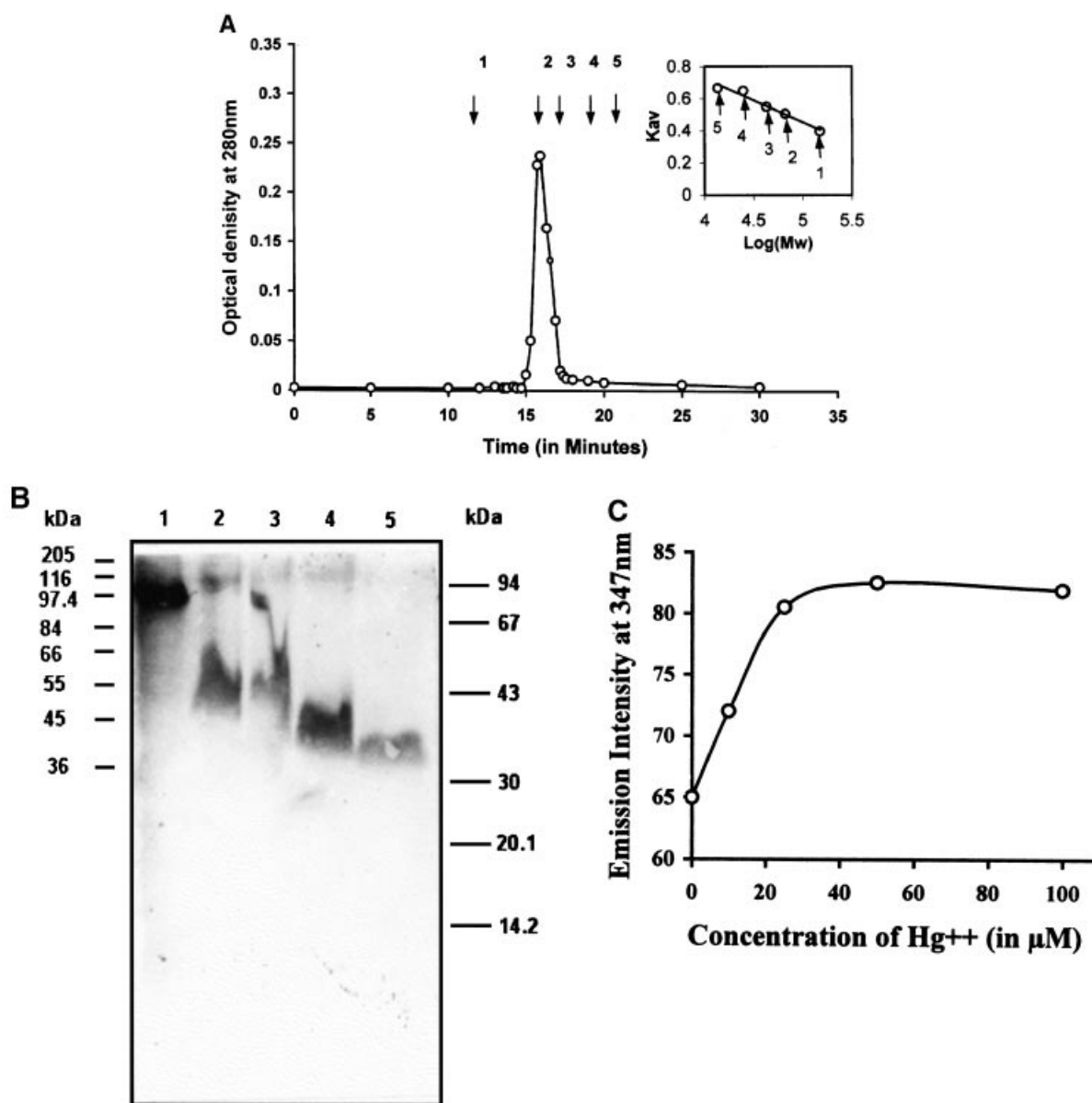
Fig. 4. Dimerization of trimeric HABP1 through Cys186. (A) Gel-permeation chromatography of cysteine-modified HABP1 (1 mg·mL^{-1}) on a Superose 6 column (1 × 30 cm) in 10 mM phosphate buffer containing 150 mM NaCl, pH 7.2, at a flow rate of 0.3 mL·min^{-1}. The column was calibrated as described in Fig. 2. (B) Pore-limiting gel electrophoresis of HABP1 and Cys186-modified HABP1. Equal amounts of HABP1 treated with 50 μM HgCl$_2$ (lane 1), native HABP1 (lane 2), modified HABP1 treated with 50 μM HgCl$_2$ (lane 3), modified HABP1 (lane 4), and SDS-treated HABP1 (lane 5) were separated on a 7–24% polyacrylamide gradient gel using 0.005% SDS in Tris/glycine running buffer, pH 8.3, as described in Materials and methods. The gel was transblotted and probed with anti-HABP1 IgG and detected using goat anti-rabbit IgG and alkaline phosphatase conjugate. (C) Change in fluorescence emission intensity at 347 nm. HABP1 was treated with various amounts of HgCl$_2$ and then desalted on a Sephadex G-25 column as described in Materials and methods.

similar conditions, in which we find the majority of the protein in the trimeric form.

There was a significant change in shape and size of HABP1 on SDS binding as well as in the presence of 2-mercaptoethanol as observed in gel-filtration experiments. It was in the monomeric state under reducing and denaturing conditions, and in the dimeric state (with a minor component of monomer) under nonreducing denaturing conditions. The reason for the predominantly dimeric form under these conditions is the oxidative atmosphere of the experiment, in which unfolded monomer becomes dimer-ized through cysteine disulfide bond formation. On the other hand, under reducing nondenaturing conditions, it is predominantly present as a trimer with a small proportion of monomer, although under native conditions, it predom-inantly remains as a trimer with a small proportion of hexamer. This clearly suggests that the trimer is stabilized through non-covalent interactions, and the formation of hexamer from trimer is facilitated by the disulfide bond formation between the subunits.

Sequence analysis confirms the presence of only one cysteine (Cys186) residue in HABP1 isolated from human
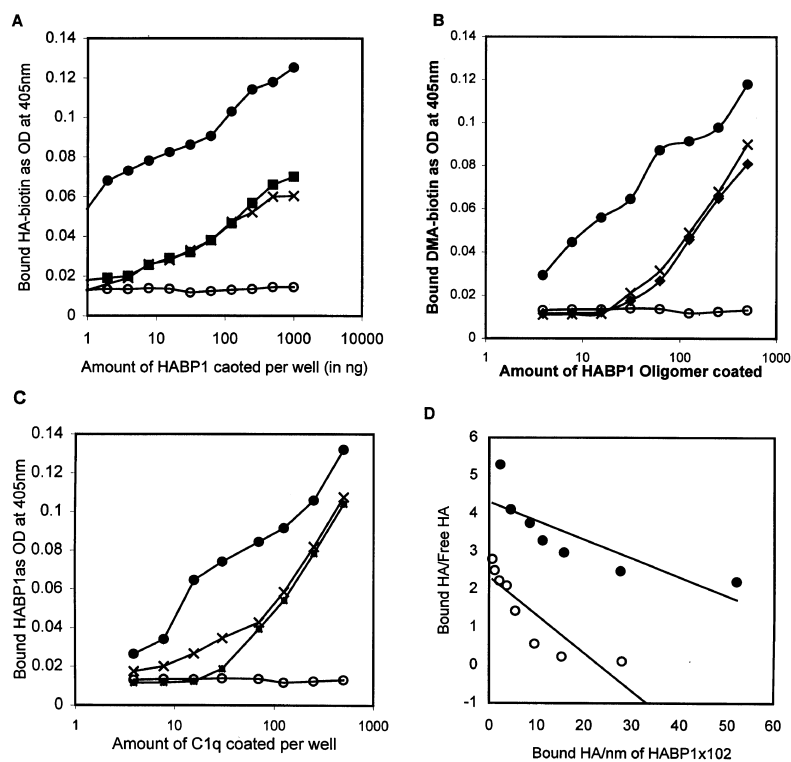
Fig. 5. Higher affinity of the hexameric form of HABP1 for its ligand. Differential ligand affinity of HABP1 oligomer purified by size-exclusion chromatography. Starting from 500 ng and using serial dilution, different oligomeric forms of HABP1 were coated on an ELISA plate in triplicate and probed with (A) biotinylated hyaluronan (HA), (B) biotinylated D-mannosylated BSA (DMA) and detected with streptavidin–horseradish peroxidase conjugate; (×) HABP1 alone; (●) HABP1 treated with 50 µM HgCl$_2$; (■) cysteine-modified HABP1 treated with HgCl$_2$; (○) BSA. (C) C1q was coated on an ELISA plate starting with 500 ng using serial dilution and incubated with different oligomeric forms of HABP1; they were then probed with rabbit anti-HABP1 IgG. The bound HABP1 was probed with alkaline phosphatase-conjugated goat anti-rabbit IgG (1 : 7500) and visualized by the 2,2′-azino-bis(3-ethylbenzthiazoline-6-sulfonic acid) detection system. (×) HABP1 alone; (●) HABP1 treated with 50 µM HgCl$_2$; (■) cysteine-modified HABP1 treated with HgCl$_2$; (○) BSA. BSA was used as negative control. Each data point is representative of three similar sets of experiment. (D) Scatchard plot analysis of the affinity of different oligomeric forms of HABP1 for hyaluronan. (○) Trimer; (●) hexamer.

and mouse [22]. Oxidation of noncovalent trimer induced by HgCl$_2$ or copper–phenanthroline shows the conversion of HABP1 into the hexameric species in buffer of low ionic strength. However, cysteine-modified HABP1 remained trimeric even after treatment with Hg^{2+} or Cu^{2+} unlike the native HABP1, clearly establishing the role of cysteine in trimer to hexamer transition. This observation is further strengthened by the absence of bound copper in the dimer of trimers of native HABP1 induced by copper–phenanthroline. Hence, it may be postulated that Cu^{2+} acts only as an oxidant and does not participate directly in dimer formation. In support of this, the higher level of trimer to hexamer association induced by HgCl$_2$ was also evident from the fluorescence analysis. HABP1 polypeptide sequences of higher eukaryotes (human and mouse) show three conserved tryptophans, of which Trp109 and Trp219 face the relatively hydrophobic side of the molecule and Trp233 resides on the negatively charged protein surface [22]. The gradual increase in fluorescence intensity of HABP1, separated by size-exclusion chromatography after pretreatment with increasing concentrations of Hg^{2+} indicates a gradual change in the microenvironment around tryptophan as the result of transition from trimer to hexamer. Dimerization of trimeric HABP1 may

lead to exposure of tryptophan to a nonpolar/hydrophobic environment, which in turn may lead to an increase in emission intensity at 347 nm [32]. In contrast with this, the crystal structure shows that Cys186 is not easily accessible for oligomerization induced by an intertrimer disulfide bond. The crystal structure of HABP1/p32 determined in the presence of 600 mM NaCl, 1 mM EGTA and 1 mM EDTA is compact compared with its form in native conditions, near pH 7.2 and physiological ionic strength. It is apparent from our observation that the hydrodynamic radius of HABP1/p32 near physiological pH and ionic strength is greater (36.2 Å) than that of the crystal structure (34.0 Å). Such an increase in hydrodynamic volume may expose Cys186 residues, enabling them to form S–S bonds.

Under native conditions, at pH 7.2, HABP1 has a hydrodynamic radius of 36.2 Å as the major species. The Cys186 residue responsible for covalent association of two trimers through disulfide bond formation is not accessible in the crystal structure. The state of HABP1 with the larger hydrodynamic radius may be different from the crystal structure, as the changes associated with the addition of trace amounts of bivalent cations may represent a structural state in which this cysteine is exposed to the solvent,

facilitating inter-trimeric disulfide bond formation. HABP1 with a larger hydrodynamic radius and solvent-exposed cysteine residue under physiological conditions may correspond to the expanded structure [33].

The existence of HABP1 in different oligomeric states has functional implications. Disulfide-mediated hexamer formation leads to a compact oligomeric structure, which is shown to have the highest ligand affinity. The monomeric form binds weakly to hyaluronan compared with the trimeric form. The low affinity of the HABP1 monomer may be explained by the presence of an additional glutamic acid residue (E127) in the putative hyaluronan-binding motif. Structural analysis of crystallographic data submitted to the protein data bank (PDB) with molecular ID 1P32, a protein that is 100% homologous with HABP1 (synonyms C1QBP, gC1qR, p32 and HABP1), reveals that the peptide segment K119 to K128 of each monomer in a trimeric assembly is usually accessible to the solvent. However, E127 of each monomer in a trimeric assembly is completely buried, as it is involved in salt bridge formation with R246 and K174 and the average distances of the two side chains of R246 and K174 from E127 are 3.2 Å and 2.8 Å, respectively. Thus, in the trimer, there are more positive charges clustering around the hyaluronan-binding motif, K119–K128. The dimerization of HABP1 trimers presumably allows multiple copies of HABP1 to interact with its ligand more strongly. However, the affinity of the dimer of trimers for D-mannosylated BSA and gC1q is similar to that of the trimer, suggesting that different mechanisms are involved in the binding of HABP1 and its different ligands. Protomer oligomerization is known to have an important role in ligand binding, signal transduction, and protein function. In the case of serum mannose-binding protein, its complement-dependent haemolytic activity is regulated by oligomeric transition [34]. Similarly, the hyaluronan-binding activity of CD44, another member of the hyaladherin family, has been linked to cellular activation. Phorbol 13-myristate 12-acetate is known to induce clustering of CD44 followed by disulfide-mediated dimerization, which is critical for binding of high levels of hyaluronan [35,36]. A similar role for cysteine-mediated oligomerization in HABP1 in signal transduction and hyaluronan binding can be expected as HABP1 is reported to be involved in hyaluronan-induced signal transduction [5–7]. So the intricate regulatory mechanism of cellular signalling by oligomerization of HABP1 may have functional implications in the cell.

REFERENCES

1. D'Souza, M. & Datta, K. (1985) Evidence of naturally occurring hyaluronic acid binding protein in rat liver. *Biochem. Int.* **10**, 43–51.

2. Gupta, S., Babu, B.R. & Datta, K. (1991) Purification, partial characterization of rat kidney hyaluronic acid binding protein and its localization on cell surface. *Eur. J. Cell Biol.* **56**, 58–67.

3. Gupta, S. & Datta, K. (1991) Possible role of hyaluronectin on cell adhesion in rat histiocytoma. *Exp. Cell Res.* **195**, 386–394.

4. Ranganathan, S., Ganguly, A.K. & Datta, K. (1994) Evidence for presence of hyaluronan binding protein on spermatozoa and its possible involvement in sperm function. *Mol. Reprod. Dev.* **38**, 69–76.

5. Ranganathan, S., Bharadwaj, A. & Datta, K. (1995) Hyaluronan mediates sperm motility by enhancing phosphorylation of proteins including hyaluronan binding protein. *Cell. Mol. Biol. Res.* **41**, 467–476.

6. Rao, C.M., Deb, T.B. & Datta, K. (1996) Hyaluronic acid induced hyaluronic acid binding protein phosphorylation and inositol triphosphate formation in lymphocytes. *Biochem. Mol. Biol. Int.* **40**, 327–337.

7. Rao, C.M., Deb, T.B., Gupta, S. & Datta, K. (1997) Regulation of cellular phosphorylation of hyaluronan binding protein and its role in the formation of second messenger. *Biochim. Biophys. Acta* **1336**, 387–393.

8. Deb, T.B. & Datta, K. (1996) Molecular cloning of human fibroblast hyaluronic acid binding protein confirms its identify with P-32, a protein co-purified with splicing factor SF2. *J. Biol. Chem.* **269**, 2206–2212.

9. Majumdar, M. & Datta, K. (1998) Assignment of cDNA encoding hyaluronic acid binding protein 1 to human chromosome 17 p12–13. *Genomics* **51**, 476–477.

10. Krainer, A.R., Mayeda, A., Kozak, D. & Binns, G. (1991) Functional expression of cloned human splicing factor SF2: homology to RNA-binding proteins, U1, 70K, and *Drosophila* splicing regulators. *Cell* **66**, 383–394.

11. Ghebrehiwet, B., Lim, B.L., Peerschke, E.I.B., Willis, C.A. & Reid, K.B.M. (1994) Isolation, cDNA cloning, and overexpression of a 33-kDa cell surface glycoprotein that binds to the globular 'Heads' of C1q. *J. Exp. Med.* **179**, 1809–1821.

12. Luo, Y., Yu, H. & Peterlin, B.M. (1994) Cellular protein modulates effects of human immunodeficiency virus type I Rev. *J. Virol.* **68**, 3850–3856.

13. Das, S., Deb, T.B., Kumar, R. & Datta, K. (1997) Multifunctional activities of human fibroblast 34-kDa hyaluronic acid-binding protein. *Gene* **190**, 223–225.

14. Soltys, B.J., Kang, D. & Gupta, R.S. (2000) Localization of P32 protein (gC1q-R.) in mitochondria and at specific extramitochondrial locations in normal tissues. *Histochem. Cell. Biol.* **114**, 245–255.

15. Brokstad, K.A., Kalland, K.H., Russell, W.C. & Matthews, D.A. (2001) Mitochondrial protein p32 can accumulate in the nucleus. *Biochem. Biophys. Res. Commun.* **281**, 1161–1169.

16. Kittlesen, D.J., Kimberly, A., Chianese-Bullock, K.A., Yao, Z.Q., Braciale, T.J. & Hahn, Y.S. (2000) Interaction between complement receptor gC1qR and hepatitis C virus core protein inhibits T-lymphocyte proliferation. *J. Clin. Invest.* **106**, 239–249.

17. Nguyen, T., Ghebrehiwet, B. & Peerschke, E.I.B. (2000) *Staphylococcus aureus* Protein A recognizes platelet gc1qR/p33: a novel mechanism for Staphylococal infection with platelets. *Infect. Immun.* **68**, 2061–2068.

18. Braun, L., Ghebrehiwet, B. & Cossart, P. (2000) gC1qR/p32, a C1q binding protein, is a receptor for the In1B invasion protein of *Listeria monocytogenes*. *EMBO J.* **19**, 1458–1466.

19. Herwald, H., Dedio, J., Kellner, R., Loos, M. & Muller-Ester, W. (1996) Isolation and characterization of the kininogen-binding protein p33 from endothelial cells. Identity with the C1q receptor. *J. Biol. Chem.* **271**, 13040–13047.

20. Kumar, R., Roychoudhary, N., Salunke, D.M. & Datta, K. (2001) Evidence for clustered mannose as a new ligand for hyaluronan binding protein (HABP1) from human fibroblast. *J. Biosci.* **26**, 325–332.

21. Simos, G. & Georgatos, S.D. (1994) The lamin B receptor-associated protein p34 shares sequence homology and antigenic determinants with the splicing factor 2-associated protein p32. *FEBS Lett.* **346**, 225–228.

22. Jiang, J., Zhang, Y., Krainer, A.R. & Xu, R.M. (1999) Crystal structure of human p32, a doughnut-shaped acidic mitochondrial matrix protein. *Proc. Natl Acad. Sci USA.* **96**, 3572–3577.

23. Lemmon, M.A. & Schlessinger, J. (1994) Regulation of signal transduction and signal diversity by receptor oligomerization. *Trends. Biochem. Sci.* **19**, 459–463.

24. Laemmli, U.K. (1970) Cleavage of structural protein during the assembly of the head of bacteriophage T4. *Nature (London)* **227**, 680–685.

25. Tyagi, R.K., Babu, B.R. & Datta, K. (1993) Simultaneous determination of native and subunit molecular weight of proteins by pore limit electrophoresis and restricted use of sodium dodecyl sulfate. *Electrophoresis* **14**, 826–828.

26. Hong, K., Ma, D., Baverley, S.M. & Turco, S.J. (2000) The *Leishmania* GDP-Mannose transporter is an autonomous multispecific hexameric complex of LPG2 subunits. *Biochemistry* **39**, 2013–2022.

27. Hollecker, M. (1990) *Protein Structure a Practical Approach.* (Creighton, T.E., eds), pp. 146–148. Oxford IRL Press, Oxford, UK.

28. Ahmad, A., Akhtar, M.S. & Bhakuni, V. (2001) Monovalent cation induced conformational change in glucose oxidase leading to stablization of enzyme. *Biochemistry* **40**, 1945–1955.

29. Kobashi, K. (1968) Catalytic oxidation of sulfhydryl groups by *o*-phenanthroline copper complex. *Biochim. Biophys. Acta* **158**, 239–245.

30. Utschig, L.M., Wright, J.G. & O'Halloran, T.V. (1993) Biochemical and spectroscopic probes of mercury(II) co-ordination environment in proteins. *Methods Enzymol.* **226**, 71–97.

31. Yang, B., Yang, B.L. & Goetinck, P.F. (1995) Biotinylated hyaluronic acid as a probe for identifying hyaluronic acid-binding proteins. *Anal. Biochem.* **228**, 299–306.

32. Maurice, R.E. (1991) Fluorescence techniques for studying protein structure. *Methods Biochem. Anal.* **35**, 127–205.

33. Reddy, G.B., Srinivas, V.R., Ahmad, N. & Surolia, A. (1999) Molten globule like state of peanut lectin monomer retains its carbohydrate specificity: implications in protein folding and legume lectin oligomerization. *J. Biol. Chem.* **274**, 4500–4503.

34. Wallis, R. & Drickamer, K. (1999) Molecular determinants of oligomer formation and complement fixation in mannose-binding proteins. *J. Biol. Chem.* **274**, 3580–3589.

35. Sleeman, J., Rudy, W., Hofmann, M., Moil, J., Herleich, P. & Ponta, H. (1996) Regulated clustering of variant CD44 proteins increases their hyaluronate binding capacity. *J. Cell Biol.* **135**, 1139–1150.

36. Liu, D. & Sy, M. (1997) Phorbol myristate acetate stimulates the dimerization of CD44 involving cysteine in transmembrane domain. *J. Immunol.* **159**, 2702–2711.